TOWARDS THE DYNAMIC PROPERTIES OF SQUARE-LATTICE QUANTUM SPIN MODELS *

Oleg Derzhko[a,b] and Taras Krokhmalskii[a]

[a]Institute for Condensed Matter Physics
1 Svientsitskii Street, L'viv-11, 79011, Ukraine

[b]Chair of Theoretical Physics, Ivan Franko National University of L'viv
12 Drahomanov Street, L'viv-5, 79005, Ukraine

(Received June 21, 2001)

Using the two-dimensional Jordan–Wigner fermionization we calculate the zz dynamic structure factor $S_{zz}(\boldsymbol{k},\omega)$ for the $s=\frac{1}{2}$ isotropic XY model on a spatially anisotropic square lattice. We discuss the dispersion relations for different modes which contribute to $S_{zz}(\boldsymbol{k},\omega)$.

PACS numbers: 75.10.–b

A study of the dynamic properties of two-dimensional (2D) quantum spin models attracts much interest during last years. Many compounds are known to be good realizations of the 2D $s=\frac{1}{2}$ Heisenberg model and the interpretation of experimental data available requires the corresponding theoretical calculations.

We consider the $s=\frac{1}{2}$ isotropic XY model (*i.e.*, XY limit of the Heisenberg model) on a spatially anisotropic square lattice governed by the Hamiltonian

$$H=\frac{1}{2}\sum_{i=0}^{\infty}\sum_{j=0}^{\infty}\left(J\left(s_{i,j}^{+}s_{i+1,j}^{-}+s_{i,j}^{-}s_{i+1,j}^{+}\right)+J_{\perp}\left(s_{i,j}^{+}s_{i,j+1}^{-}+s_{i,j}^{-}s_{i,j+1}^{+}\right)\right) \tag{1}$$

($J\geq 0$ and $J_{\perp}\geq 0$ are the exchange interactions between the neighbouring sites in a row and in a column, respectively) and calculate the zz dynamic structure factor

$$\begin{aligned}S_{zz}(\boldsymbol{k},\omega) \;=\; & \sum_{p=0}^{\infty}\sum_{q=0}^{\infty}\mathrm{e}^{i(k_xp+k_yq)}\int_{-\infty}^{\infty}dt\mathrm{e}^{i\omega t}\left(\langle s_{n,m}^{z}(t)s_{n+p,m+q}^{z}\rangle\right.\\ & \left.-\langle s_{n,m}^{z}\rangle\langle s_{n+p,m+q}^{z}\rangle\right)\end{aligned} \tag{2}$$

* Presented at the XII School of Modern Physics on Phase Transitions and Critical Phenomena, Lądek Zdrój, Poland, June 21–24, 2001.

(the angular brackets in (2) denote the canonical thermodynamic average with the Hamiltonian (1)). To obtain the desired quantity we use the 2D Jordan–Wigner fermionization and adopt a mean-field treatment of the phase factors which appear after the fermionization of the spin Hamiltonian (1) (an approximate step) (see [1] and also [2] for a brief review). As a result we face a model of tight-binding spinless fermions on a square lattice. Performing the Bogolyubov transformation we present the spin model (1) as spinless fermions governed by the Hamiltonian

$$H = \sum_{\boldsymbol{k}}{}' \Lambda_{\boldsymbol{k}} \left(\alpha_{\boldsymbol{k}}^{+}\alpha_{\boldsymbol{k}} - \beta_{\boldsymbol{k}}^{+}\beta_{\boldsymbol{k}}\right), \; \Lambda_{\boldsymbol{k}} = \sqrt{J^2 \sin^2 k_x + J_{\perp}^2 \cos^2 k_y} \geq 0 \qquad (3)$$

($\alpha_{\boldsymbol{k}}^{+}$, $\alpha_{\boldsymbol{k}}$, $\beta_{\boldsymbol{k}}^{+}$, $\beta_{\boldsymbol{k}}$ obey the Fermi commutation rules, the prime in (3) denotes that $\boldsymbol{k}$ varies in the region $-\pi \leq k_x \leq \pi$, $-\pi + |k_x| \leq k_y \leq \pi - |k_x|$). Rewriting the time-dependent zz spin correlation function involved into (2) in terms of spinless fermions, using the Wick–Bloch–de Dominicis theorem and performing the Fourier transformations with respect to time and site variables we find the following result for the zz dynamic structure factor

$$\begin{aligned} S_{zz}(\boldsymbol{k},\omega) &= \pi \int_{-\pi}^{\pi} \frac{dk_{1x}}{2\pi} \int_{-\pi}^{\pi} \frac{dk_{1y}}{2\pi} \\ &\times \Bigg(\cos^2 \frac{\gamma_{\boldsymbol{k}_1+\boldsymbol{k}} - \gamma_{\boldsymbol{k}_1}}{2} \Big(n_{\boldsymbol{k}_1} \left(1 - n_{\boldsymbol{k}_1+\boldsymbol{k}}\right) \delta\left(\omega + \Lambda_{\boldsymbol{k}_1} - \Lambda_{\boldsymbol{k}_1+\boldsymbol{k}}\right) \\ &+ \left(1 - n_{\boldsymbol{k}_1}\right) n_{\boldsymbol{k}_1+\boldsymbol{k}} \delta\left(\omega - \Lambda_{\boldsymbol{k}_1} + \Lambda_{\boldsymbol{k}_1+\boldsymbol{k}}\right)\Big) \\ &+ \sin^2 \frac{\gamma_{\boldsymbol{k}_1+\boldsymbol{k}} - \gamma_{\boldsymbol{k}_1}}{2} \Big(n_{\boldsymbol{k}_1} n_{\boldsymbol{k}_1+\boldsymbol{k}} \delta\left(\omega + \Lambda_{\boldsymbol{k}_1} + \Lambda_{\boldsymbol{k}_1+\boldsymbol{k}}\right) \\ &+ \left(1 - n_{\boldsymbol{k}_1}\right)\left(1 - n_{\boldsymbol{k}_1+\boldsymbol{k}}\right) \delta\left(\omega - \Lambda_{\boldsymbol{k}_1} - \Lambda_{\boldsymbol{k}_1+\boldsymbol{k}}\right)\Big)\Bigg). \end{aligned} \qquad (4)$$

Here $\cos\frac{\gamma_{\boldsymbol{k}}}{2} = \sqrt{\frac{1}{2} + \frac{J_{\perp}\cos k_y}{2\Lambda_{\boldsymbol{k}}}}$, $\sin\frac{\gamma_{\boldsymbol{k}}}{2} = \mathrm{sgn}\left(J \sin k_x\right) \sqrt{\frac{1}{2} - \frac{J_{\perp}\cos k_y}{2\Lambda_{\boldsymbol{k}}}}$, and $n_{\boldsymbol{k}} = \frac{1}{\mathrm{e}^{\beta\Lambda_{\boldsymbol{k}}}+1}$ is the Fermi factor.

In Fig. 1 and Fig. 2 we display the greyscale plots of $S_{zz}(\boldsymbol{k},\omega)$ (4) for the square-lattice $s=\frac{1}{2}$ isotropic XY model (with $J_{\perp}=J$ and $J_{\perp}=0.1J$) at zero temperature $\beta=\infty$ and at high temperature $\beta=0.1$, respectively. As it follows from (4) the zz dynamic structure factor of the square-lattice $s=\frac{1}{2}$ isotropic XY model within the frames of the exploited approach is governed by a continuum of two Jordan-Wigner fermions. On the basis of (4) one can easily compose two-fermion excitations for which $S_{zz}(\boldsymbol{k},\omega)$ exhibits peaks, cusps, cutoffs which can be seen in Figs. 1, 2.

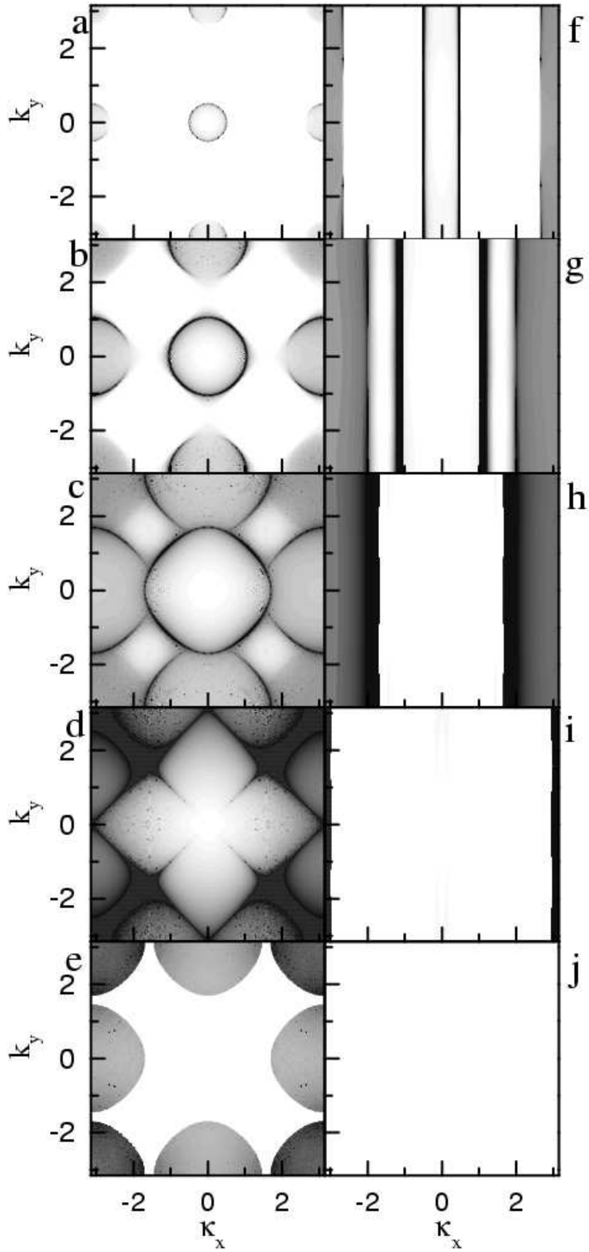

Fig. 1. $S_{zz}(\boldsymbol{k},\omega)$ at zero temperature $\beta=\infty$ for the 2D $s=\frac{1}{2}$ isotropic XY model (1) as it follows from (4). $J = J_{\perp} = 1$ (a – e), $J = 0.1\, J_{\perp} = 1$ (f – j), $\omega = 0.5$ (a, f), $\omega = 1$ (b, g), $\omega = 1.5$ (c, h), $\omega = 2$ (d, i), $\omega = 2.5$ (e, j).

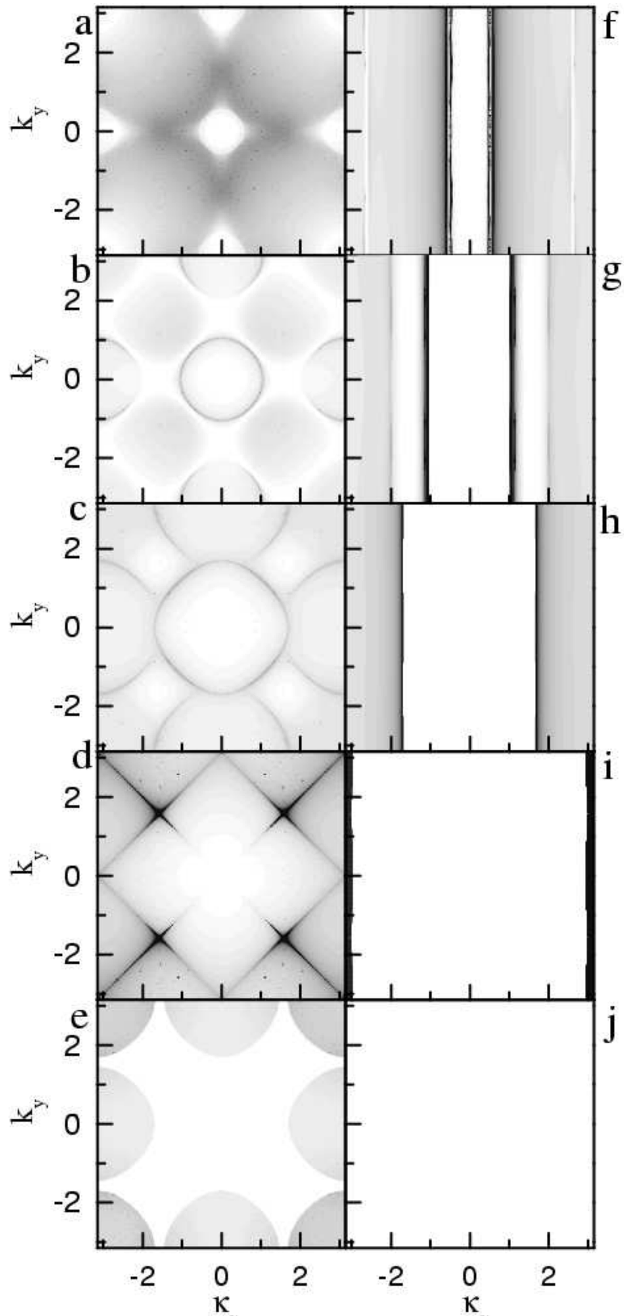

Fig. 2. The same as in Fig. 1 at high temperature $\beta = 0.1$.

Namely,

(1) the well-known spin wave [3], which is composed of two fermions with $\boldsymbol{k}_1 = \left(0, \frac{\pi}{2}\right) - \frac{\boldsymbol{k}}{2}$ and $\boldsymbol{k}_1 + \boldsymbol{k} = \left(0, \frac{\pi}{2}\right) + \frac{\boldsymbol{k}}{2}$ with the energy of the pair

$$\omega_{\boldsymbol{k}} = 2\sqrt{J^2 \sin^2 \frac{k_x}{2} + J_\perp^2 \sin^2 \frac{k_y}{2}} \tag{5}$$

or of two fermions with $\boldsymbol{k}_1 = \left(\frac{\pi}{2}, 0\right) - \frac{\boldsymbol{k}}{2}$ and $\boldsymbol{k}_1 + \boldsymbol{k} = \left(\frac{\pi}{2}, 0\right) + \frac{\boldsymbol{k}}{2}$ with the energy of the pair

$$\omega_{\boldsymbol{k}} = 2\sqrt{J^2 \cos^2 \frac{k_x}{2} + J_\perp^2 \cos^2 \frac{k_y}{2}}; \tag{6}$$

(2) the high-frequency modes ($\boldsymbol{k}_1 = -\frac{\boldsymbol{k}}{2}$, $\boldsymbol{k}_1 = \left(\frac{\pi}{2}, \frac{\pi}{2}\right) - \frac{\boldsymbol{k}}{2}$) with the dispersion relations

$$\omega_{\boldsymbol{k}} = 2\sqrt{J^2 \sin^2 \frac{k_x}{2} + J_\perp^2 \cos^2 \frac{k_y}{2}}, \tag{7}$$

$$\omega_{\boldsymbol{k}} = 2\sqrt{J^2 \cos^2 \frac{k_x}{2} + J_\perp^2 \sin^2 \frac{k_y}{2}}; \tag{8}$$

(3) another high-frequency modes $\left(\boldsymbol{k}_1 = 0,\ \boldsymbol{k}_1 = \left(\frac{\pi}{2}, \frac{\pi}{2}\right)\right)$ with the dispersion relations

$$\omega_{\boldsymbol{k}} = J_\perp + \sqrt{J^2 \sin^2 k_x + J_\perp^2 \cos^2 k_y}, \tag{9}$$

$$\omega_{\boldsymbol{k}} = J + \sqrt{J^2 \cos^2 k_x + J_\perp^2 \sin^2 k_y}; \tag{10}$$

(4) the low-frequency mode ($\boldsymbol{k}_1 = \left(0, \frac{\pi}{2}\right)$) with the dispersion relation

$$\omega_{\boldsymbol{k}} = \sqrt{J^2 \sin^2 k_x + J_\perp^2 \sin^2 k_y}; \tag{11}$$

(5) the low-frequency modes which become visible only as the temperature increases (at zero temperature they are forbidden because of the Fermi factors in (4)) (compare Figs. 1a, 1f and Figs. 2a, 2f).

The established modes (5)–(11) manifest themselves as peaks, cusps or cutoffs in the wave vector profiles of $S_{zz}(\boldsymbol{k}, \omega)$ (the constant frequency scans of $S_{zz}(\boldsymbol{k}, \omega)$) and may be used for a precise determining of the Hamiltonian parameters J and $J_\perp$ from the dynamic experiment data on 2D $s = \frac{1}{2}$ isotropic XY compounds.

It should be stressed that Eq. (4) contains the exact result in the 1D limit [4] which emerges after putting $J_\perp = 0$ or $J = 0$. On the other hand, Eq. (4) is not the rigorous expression for $S_{zz}(\boldsymbol{k},\omega)$ because of the mean-field description of the phase factors which arise after fermionization. Within the adopted treatment we have neglected the complicated interaction between spinless fermions. In the case of the isotropic Heisenberg model the interaction between spinless fermions is present even within the adopted mean-field procedure because of the Ising interaction of z spin components. The quartic terms in the fermion Hamiltonian can be treated after making further approximation (see [1, 2]). It seems obvious to extend the present investigation to a study of the square-lattice $s = \frac{1}{2}$ isotropic Heisenberg model which is used for interpreting the experimental data for a number of compounds.

To summarize, we have presented the first results for the zz dynamic structure factor of the $s = \frac{1}{2}$ isotropic XY model on a spatially anisotropic square lattice derived on the basis of the 2D Jordan–Wigner fermionization. Our study has indicated excitations which govern the zz dynamic structure factor and may be useful for understanding the dynamic experiments for corresponding 2D magnetic materials.

The paper was discussed at the University of Wrocław. O. D. is grateful to J. Jędrzejewski for the hospitality at the University of Wrocław in the Spring of 2001.

REFERENCES

[1] Y.R. Wang, *Phys. Rev.* **B43,** 3786 (1991).

[2] O. Derzhko, *J. Phys. Stud.* (L'viv) **5**, 49 (2001).

[3] G. Gomez-Santos, J.D. Joannopoulos, *Phys. Rev.* **B36,** 8707 (1987).

[4] G. Müller, H. Thomas, H. Beck, J.C. Bonner, *Phys. Rev.* **B24,** 1429 (1981); J.H. Taylor, G. Müller, *Physica* **A130,** 1 (1985).